

# Transmission of keV $O^-$ ions through a single tapered glass capillary

P. Pan, S.T. Niu, H.Y. Song, X.M. Chen, X.Y. Qiu\*, J.X. Shao\*

School of Nuclear Science and Technology, Lanzhou University, Lanzhou 730000, China

## ARTICLE INFO

### Keywords:

Transmission  
Tapered glass capillary  
Negative ions  
Focusing

## ABSTRACT

An experimental study of 14 keV  $O^-$  ions transmission through a tapered glass capillary with the inlet diameters of 580  $\mu m$ , an outlet diameter of 68  $\mu m$  and a length of 45 mm, has been performed in this work. It indicates that the  $O^-$  ions transmitting through the tapered capillary had a density enhancement of about 5.5 times with the tilt angle of  $0^\circ$ . It was found that more than 97% of the transmitted and focused ions remained their initial charge state in central area. It's the first time that focusing effect was observed and was reported in experiment for negative ions. The angular distribution of transmitted ions was narrow. These results clearly indicated that the focusing effect can be achieved in the transmission process of keV  $O^-$  ions through a tapered glass capillary.

## 1. Introduction

The study of applying tapered glass capillary to generate negative focused ion beam (FIB) is a fairly attractive research subject on account of its potential use in material science and technology. When the negative ions were implanted into an insulated or semi-conducting material, high precision can be achieved via micro-size tapered glass capillary in the implantation process. Therefore, FIB technique can be applied to the surface modification of nanostructured materials [1]. In Mehta's work, FIB was implanted into the surface of a thin insulator film and then nanometer particles were deposited to manipulate and fabricate quantum devices at the nanoscale [2]. Furthermore, a primary focused negative oxygen ion beam was used to generate secondary positive ions in secondary ion mass spectrometry (SIMS) instrument for biological samples analysis [3]. The simple focusing instruments for low energy ion beams was rapidly developed in recent years.

The pioneering work, the transmission of 3 keV  $Ne^{7+}$  through polyethylene terephthalate (PET) nano-capillaries based on the guiding effect, has been reported by N. Stolterfoht et al. [4]. During the whole process of transmission, self-organized charge patches were deposited inside the glass capillary and the transmission achieved dynamic equilibrium, which led to the formation of electric field. Furthermore, this verified that highly charged ions (HCIs) remained in the initial charge state without charge exchange. Surprisingly, the beam could still exit along the axis of capillary until the tilt angle was as large as  $\pm 25^\circ$ . For the case that negative ions transmit through nano-capillaries, it has been reported that charge deposition on the inner wall of capillary is insufficient in our previous work [5,6].

In recent years, the tapered glass capillary has been developed to

obtain a micro-beam, even a nano-beam, using the manufacturing technology of micro- and macro-capillaries [7–12]. As for  $H^+$  at the energy of several MeV, focusing factors of about 1.6–2.4 based on small-angle scattering by the inner wall of tapered capillary were reported [13]. Several studies have already reported that the transmission of HCIs through tapered glass capillary attributes to the guiding effect [7–9,11] and the focusing factor is as high as  $\sim 7$  for the 8 keV  $Ar^{8+}$  with incident current of 0.2 pA [7,14]. However, up to now, the transmission of negative ions through single glass capillary has not been reported experimentally or theoretically. Thus, more investigations are needed to explore the focusing mechanism for low energy negative ions.

We investigate the transmission process of 14 keV  $O^-$  ions through a single glass capillary in this work. The result indicates that macroscopic tapered capillary can be used to focus negative ion beam, on account of the electric potential on the inner surface of insulating capillary [15,16].

## 2. Experimental setup

The experiment was performed at the  $2 \times 1.7$  MV Tandem Electrostatic Accelerator Laboratory of Lanzhou University. The operating pressure in the chamber is superior to  $5.0 \times 10^{-6}$  Pa. The continuous ion beam is extracted from the sputter-type negative ion source at the electrical potential of 14 kV. Then, the beam was collimated by two sets of collimators (which were 75 cm apart from each other) of  $1.5 \times 1.5$  mm<sup>2</sup> before entering a vacuum chamber. The angular divergence of incident beam was about  $0.2^\circ$  in the whole measuring process. The experimental set-up was shown in Fig. 1. The tapered borosilicate glass capillary (with the length of 45 mm, inlet diameter of 580  $\mu m$  and

\* Corresponding authors at: School of Nuclear Science and Technology, Lanzhou University, South Tianshui Road No. 222, Lanzhou City 730000, China.  
E-mail address: [Panp17@lzu.edu.cn](mailto:Panp17@lzu.edu.cn) (P. Pan).

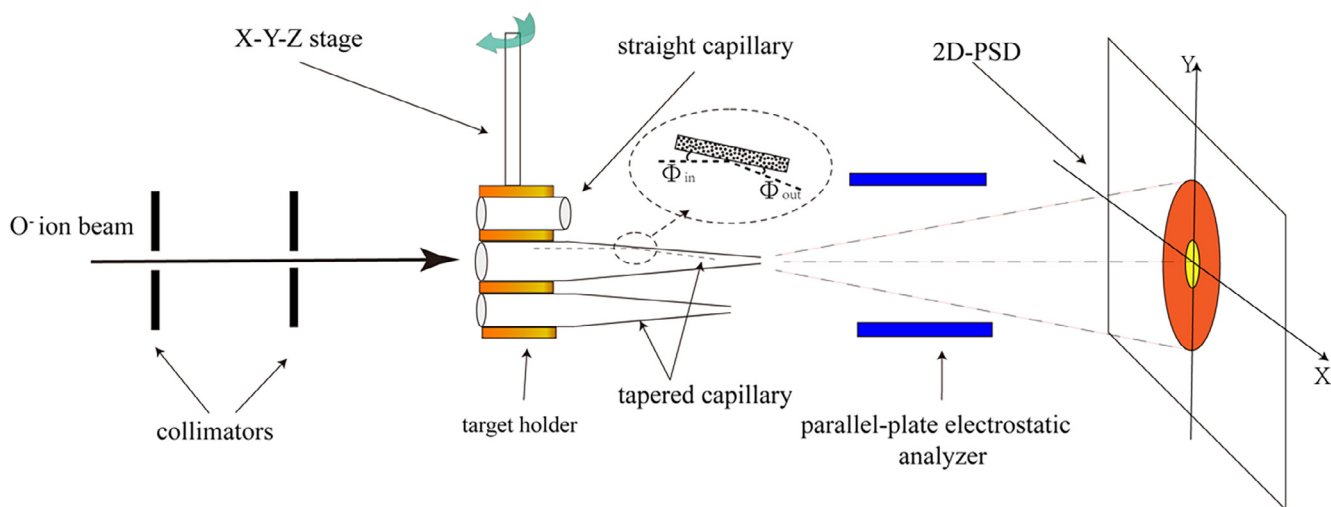


Fig. 1. Schematic view of the experimental setup (Not to scale).

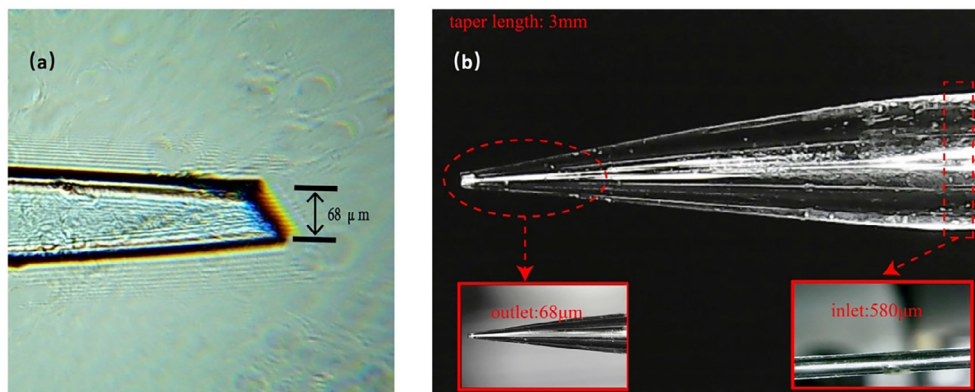


Fig. 2. Picture of the tapered glass capillary with inner diameters of the inlet ( $\phi_{in} = 580 \mu\text{m}$ ) and outlet ( $\phi_{out} = 68 \mu\text{m}$ ). The total length of the capillary is 45 mm and the tapered part is  $\sim 3$  mm. On the left side of the picture above is the microscopy image of capillary tip.

outlet diameter of  $68 \mu\text{m}$ ) used in the experiment was prepared at our laboratory. It was fabricated by heating a straight borosilicate glass (composed of 81%  $\text{SiO}_2$ , 13%  $\text{B}_2\text{O}_3$ , 4%  $\text{Na}_2\text{O}$ , 2%  $\text{Al}_2\text{O}_3$  and other constituents) tube with the inner diameter of  $580 \mu\text{m}$ , and was fixed and stretched afterwards by pulling both ends of the tube with a constant force. The heating temperature of this kind of borosilicate glass is about  $815^\circ\text{C}$ . The dimensions of the tapered capillary sample were shown in Fig. 2.

The target can be rotated around the vertical/horizontal axis, it could also be moved in the directions of x, y and z with high accuracy. The charge states of transmitted ions were analyzed by a pair of parallel-plate electrostatic analyzers located about 5 cm downstream from the capillary. Then, a two-dimensional position-sensitive micro-channel plate detector (2D-PSD) was located at the end of the experimental setup to record the number and position of transmitted particles. As shown in Fig. 1,  $\psi_{in}$  is the tilt angle between the incident beam and the X direction of the capillary,  $\psi_{out}$  is the output angle between the scattering direction of transmitted particles impacted on the detector and the incident direction of primary beam. We determined the  $0^\circ$  position by adjusting the vertical and horizontal parameters in an angle adjuster to reach the maximum counting rate, when the largest number of particles passed through capillary directly without any collision occurred at close range. At the  $0^\circ$  position the tilt angle  $\psi_{in}$  is  $0^\circ$ . Small angular step of the angle adjuster made the accuracy of the  $0^\circ$  position to be very small (about  $0.02^\circ$ ).

The tapered glass capillary was installed in the center of UHV chamber. Our target holder can hold three parallel tubes at the same

time. One of them was a straight tube as an experimental control group to measure the density of ions that were injected into the tapered capillary. Here, the inlet diameter of tapered capillary is the same as that of straight capillary. It was supposed that the counting rate of ions coming out from straight capillary was equal to that of ions injected into tapered capillary. We calculated the focusing factor  $\sigma$  of transmitted ion beam by Eq. (1):

$$\sigma = \frac{\bar{J}_{out}}{\bar{J}_{in}} = \frac{\bar{R}_{out}/S_{out}}{\bar{R}_{in}/S_{in}} \quad (1)$$

Here,  $\bar{J}_{out}$  and  $\bar{J}_{in}$  are the average current densities of output and input respectively,  $S_{out}$  and  $S_{in}$  are areas of the cross section of the outlet and inlet,  $\bar{R}_{out}$  and  $\bar{R}_{in}$  are the average counting rates of tapered and straight capillaries recorded by the 2D-PSD.

We measured the purities (fraction of  $\text{O}^-$ ,  $\text{N}(\text{O}^-)/\text{N}(\text{O}^- + \text{O}^0)$ ) of transmitted  $\text{O}^-$  through straight capillary and tapered capillary, respectively. We ensure that the projectiles would not be deflected out of the effective area of micro-channel plate detector by applying an identical voltage ( $\pm 200$  V) to the electrostatic analyzer. Thus, particles (negative, positive or neutral) with different charge states were separated by parallel electric field and then all the particles were recorded by the detector simultaneously. This kind of charge analyzer deflected the ions along the Y axis but not along the X axis. The 2D-PSD could be used to measure angular distribution of transmitted particles. A multi-parameter acquisition system (MPA-3) and its corresponding software (FAST ComTec) were used for data acquisition and data analysis.

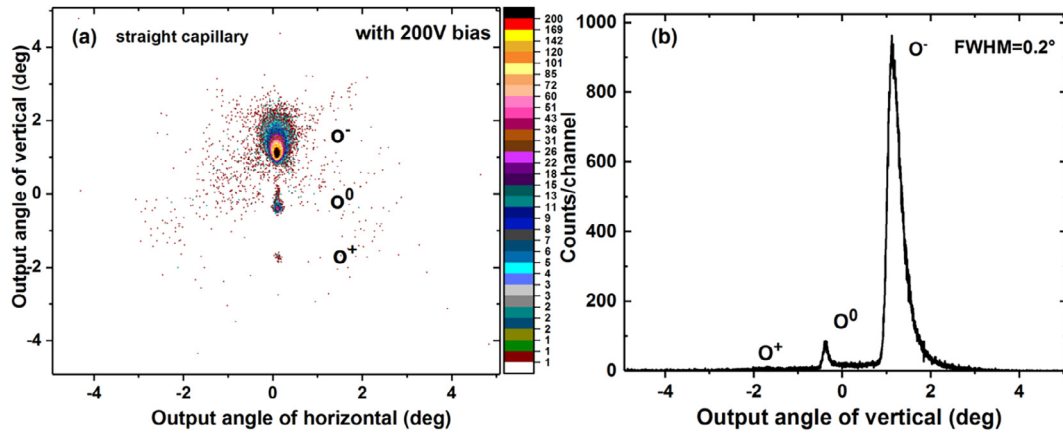


Fig. 3. (a) The typical 2D plot of transmission and distribution of 14 keV  $O^-$  ions through a straight glass capillary (inner diameter of 580  $\mu\text{m}$ , length of 33 mm) with  $0^\circ$  incident angle and bias voltage ( $\pm 200$  V), a small dot on the map represents a particle. (b) The projection of (a) in the vertical direction.

### 3. Results and discussion

Fig. 3(a) reflects the 2D angular distribution of 14 keV  $O^-$  ions transporting through the straight capillary. Besides, because of the divergence of primary projectiles impacting with inner wall of capillary, three kinds of particles ( $O^-$ ,  $O^0$ , and  $O^+$ ) were observed. Fig. 3(b) shows the projection of Fig. 3(a) in the vertical axis. The fractions of  $O^0$  and  $O^+$  ions are significantly lower than that of  $O^-$  ions, so these can be neglected in the experiment. The profile width (FWHM) is  $0.2^\circ$  in vertical direction which is close to angular divergence of primary projectiles. These results imply that the projectiles injected into

capillary at the tilted angle of  $0^\circ$ .

As shown in Fig. 4(a), the typical 2D image of 14 keV  $O^-$  transmitted through a tapered glass capillary ( $\phi_{\text{out}} = 68 \mu\text{m}$ ) is recorded by the 2D-PSD. Fig. 4(b) and (c) show the projections of Fig. 4(a) in horizontal and vertical directions respectively. For focused ion beam, it was showed that in the case of zero tilt angle, most of the outgoing particles did not loss electrons when interplaying with the inner wall of glass capillary. Most of the negative ions survived after being electrostatically scattered from the inner surface of insulated tapered glass capillary. As shown in Fig. 4(d), the purity of  $O^-$  is not less than 97%, which means that most of the negative ions did not have charge

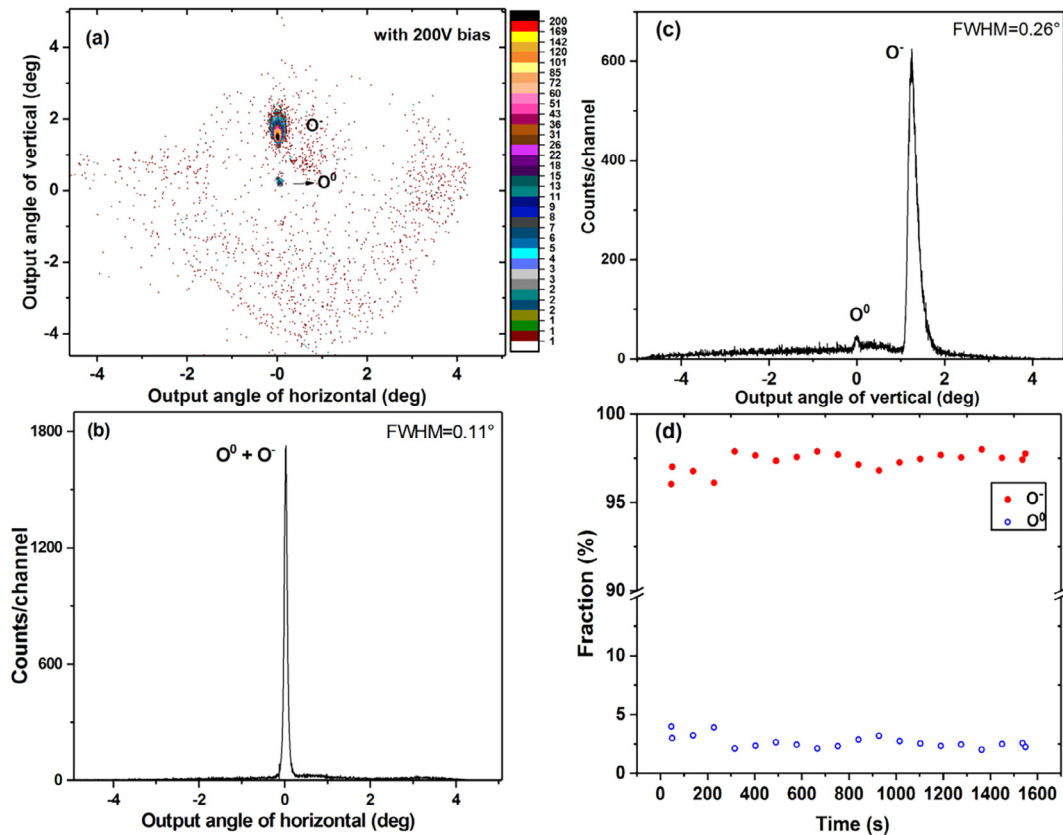
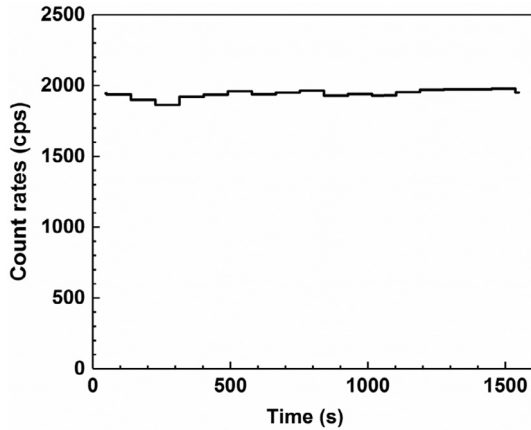


Fig. 4. Picture (a), the typical 2D plot of transmission and distribution of 14 keV  $O^-$  ions through a tapered glass capillary (diameter of 68  $\mu\text{m}$ , length of 4.5 cm) with  $0^\circ$  tilted angle and bias voltage ( $\pm 200$  V), then recorded by the 2D-PSD. A small dot on the map represents a particle. (b) and (c) Is the projection of (a) in the direction of horizontal and vertical respectively. The profile width (represents by FWHM) of transmitted beam is narrow ( $0.11^\circ$  and  $0.26^\circ$ , respectively). (d) The proportion of  $O^-$  ions (solid dots) and  $O^+$  ions (hollow dots) traveled through tapered capillary as a function of time.



**Fig. 5.** The average count rates of 14 keV  $O^-$  ions transmitted through tapered glass capillary as a function of time. We obtain dates within per  $\sim 90$  s. The stability of  $O^-$  ion current is better than  $1 \pm 3\%$  during the measurement time of 1500 s. The counts at the 2D-PSD were corrected to be divided by the detection efficiency of 55%.

exchange at the tilt angle of  $0^\circ$ .

For scattering events of charged particle under the situation of grazing incidence, any macroscopic charging up phenomena on the surface of insulated targets should be taken into consideration. The interplay mechanism between ions and the inner wall of capillary is roughly the same as that between ions and the surface of plane. High fractions of negative ions could also be observed in the case of grazing scattering between ions and the insulated surface in other related works [17,18]. As shown in Fig. 1, the tilt angle of zero on the inner wall could also be seemed as that on the surface of a plane to some extent in the situation of glancing incidence, therefore, the perpendicular energy  $E_\perp$  of incident ion could be expressed as Eq. (2):

$$E_\perp = E_0 \sin^2 \Phi_{in} \quad (2)$$

where  $\Phi_{in}$  (as seen in Eq. (3)) is the incident angle of projectiles with respect to inner wall of capillary,  $\theta_{taper}$  is the taper angle of capillary.

$$\Phi_{in} = \frac{\theta_{taper}}{2} \quad (3)$$

The analysis of the data is straightforward. Here,  $\theta_{taper}$  is less than  $2^\circ$ . For the  $O^-$  ions with the kinetic energy of 14 keV, we roughly estimate that the average tapered angle at the tip of the capillary,  $\Phi_{in}$ , is less than  $1^\circ$ . Therefore, it could be obtained that  $E_\perp$  4 eV. The energy of  $E_\perp$  is also comparable with that of the surface potential energy  $qU$  ( $\sim 4$  eV) of the inner wall (made of  $SiO_2$ ) due to charging effect [15]. Therefore, it can be believed that the projectiles did not overcome the repulsive potential of the inner surface and were reflected in front of the surface.

It was observed that the 14 keV  $O^-$  ions transmitting through the tapered glass could be divided into two different components: a)  $O^-$  ions remaining their original charge states after traveling through the capillary. These  $O^-$  ions were represented by intense spots in the center of the image. b)  $O^-$  ions being neutralized in the progress of being scattered by the capillary inner surface. Those ions were represented by randomly distributed dots in Fig. 4(a). In this study, we use ‘core’ and ‘halo’ to denote the former and the latter, respectively. A similar pattern has also been reported in the study of MeV protons transporting through tapered glass capillary [13]. In contrast, it is the core component rather than the halo component dominantly contribute to the beam focusing effect of the tapered glass capillary in this work. For primary ion beam in the motion process with the energy of keV, the perpendicular energy  $E_\perp$  is of the order of eV. Whereas, for those with the energy of MeV, the perpendicular energy is about 3 orders of magnitude greater than that for keV primary ion beam. Thus, primary projectiles of MeV with the perpendicular energy of keV can overcome

**Table 1**

Counting rate and ion density of the transmitted beams of  $O^-$  ions through tapered glass capillary with a kinetic energy of 14 keV.

	Incident ion beam	Transmitted ion beam	Focusing factor
Counts at PSD	25,300 cps	1940 cps	
Ion density	$9.7 \times 10^4$ cps/mm <sup>2</sup>	$5.4 \times 10^5$ cps/mm <sup>2</sup>	5.5

the repulsive potential of the surface and then transport via multiple stochastic binary encounters below surface. The mechanism of the transmission has been discussed in detail in our previous work [19].

The measurement during the course of the experiment is continuous to analyze the current stability of the transmitted  $O^-$  ions beam. As shown in Fig. 5, the line represents an averaged counting rates of every 90 s. It was seen that the current of transmitted  $O^-$  ions is relatively stable ( $\sim 2000$  cps). In the course of the measurement, the stability of current is about 3%. The stable transmitted current inside the capillary was established in a very short time. Furthermore, the transmission intensity through straight capillary projectiles kept below  $0.1$  pA/mm<sup>2</sup> to avoid the saturation of MCP counts (accompanied with the overlarge dead time) and the distortion of data [20]. It is noted that the low density of projectiles achieved dynamic balance within short time and then the interplay did not evolve with time. Table 1 lists the counting rate and ion density of the transmitted beams of 14 keV  $O^-$  ions through the tapered glass capillary. It indicates that the ion current density was increased by a factor of 5.5 after transmission.

#### 4. Conclusion

The experimental study on the transportation of low energy  $O^-$  ions through a single tapered glass capillary was reported in this work. By using the capillary (with outlet diameter of  $68 \mu\text{m}$ ), the stable transmission of  $O^-$  ions with a focusing factor of approximate 5.5 was observed. The transmitted particles could be mainly divided into two parts: these ions transmitted directly and those ions scattered by the inner wall of capillary. We find that the central part (‘core’) dominantly contributed to the beam focusing effect with the tapered glass capillary and that the percentage of  $O^-$  ions was higher than 97% in the central area. Therefore, it was suggested that charge deposition and electrostatic scattering dominated the transport process of negative ions with the beams intensity of under several pA/mm<sup>2</sup> in small angle scattering. These results indicate that the focusing effect can also be achieved in the transmission progress of keV  $O^-$  through a tapered glass capillary at the tilt angle of  $0^\circ$ .

#### Acknowledgments

The authors are grateful to M.L. Sun for helpful discussions. This work was supported by the National Natural Science Foundation of China (Grants No. 11675067, No. 11775103 and No. 11605078). The authors also thank the IAEA financial support for the 23<sup>rd</sup> IBA conference.

#### References

- [1] A.V. Krashennnikov, F. Banhart, Engineering of nanostructured carbon materials with electron or ion beams, *Nat. Mater.* 6 (10) (2007) 723–733.
- [2] M. Mehta, et al., Focused ion beam implantation induced site-selective growth of InAs quantum dots, *Appl. Phys. Lett.* 91 (12) (2007) 123108.
- [3] S.G. Boxer, M.L. Kraft, P.K. Weber, Advances in imaging secondary ion mass spectrometry for biological samples, *Annu. Rev. Biophys.* 38 (2009) 53–74.
- [4] N. Stollerfoht, et al., Transmission of 3 keV  $Ne^+$  ions through nanocapillaries etched in polymer foils: evidence for capillary guiding, *Phys. Rev. Lett.* 88 (13) (2002) 133201.
- [5] G. Sun, et al., Interaction of 18-keV  $O^-$  ions with  $Al_2O_3$  nanocapillaries, *Phys. Rev. A* (2009) 79(5).
- [6] D. Feng, et al., Dynamic guiding process of 10-keV  $O^-$  ions transmitting through  $Al_2O_3$  nanocapillaries, *Phys. Rev. A* (2012) 85(6).

- [7] T. Ikeda, et al., Production of a microbeam of slow highly charged ions with a tapered glass capillary, *Appl. Phys. Lett.* 89 (16) (2006) 163502.
- [8] R.J. Berezky, et al., Transmission of 4.5 keV ions through a single glass macrocapillary, *Nucl. Instrum. Methods Phys. Res. Sect. B* 267 (2) (2009) 317–320.
- [9] M. Kreller, G. Zschornack, U. Kentsch, Guiding of argon ions through a tapered glass capillary, *Nucl. Instrum. Methods Phys. Res. Sect. B* 269 (9) (2011) 1032–1035.
- [10] J. Chen, et al., Focusing of 90keV O<sup>6+</sup> ions through a single tapered glass macrocapillary, *Nucl. Instrum. Methods Phys. Res. Sect. B* 281 (2012) 26–29.
- [11] G. Kowarik, et al., Production of a microbeam of slow highly charged ions with a single microscopic glass capillary, *Nucl. Instrum. Methods Phys. Res. Sect. B* 267 (12–13) (2009) 2277–2279.
- [12] S.J. Wickramarachchi, et al., Electron transmission through a microsize tapered glass capillary, *Nucl. Instrum. Methods Phys. Res. Sect. B* 269 (11) (2011) 1248–1252.
- [13] J. Hasegawa, et al., Transport mechanism of MeV protons in tapered glass capillaries, *J. Appl. Phys.* 110 (4) (2011).
- [14] N. Stolterfoht, Y. Yamazaki, Guiding of charged particles through capillaries in insulating materials, *Phys. Rep.* 629 (2016) 1–107.
- [15] H. Tsuji, Y. Gotoh, J. Ishikawa, Secondary electron emission and surface potential of SiO<sub>2</sub> film surface by negative ion bombardment, *Nucl. Instrum. Methods Phys. Res. Sect. B* 141 (1–4) (1998) 645–651.
- [16] E. Giglio, et al., Evolution of the electric potential of an insulator under charged particle impact, *Phys. Rev. A* 95 (3) (2017) 030702.
- [17] C. Auth, A.G. Borisov, H. Winter, High fractions of negative ions in grazing scattering of fast oxygen atoms from a LiF(100) surface, *Phys. Rev. Lett.* 75 (12) (1995) 2292–2295.
- [18] S. Ustaze, et al., Electron capture and loss processes in the interaction of hydrogen, oxygen, and fluorine atoms and negative ions with a MgO(100) surface, *Phys. Rev. Lett.* 79 (18) (1997) 3526–3529.
- [19] G.Y. Wang, et al., Transmission of hundred-keV protons through insulating nanocapillaries: charge-patch-assisted specular reflections, *Sci. Rep.* 5 (2015) 15169.
- [20] J. Zhao, et al., Application of position sensitive detector for the electron detachment cross-sections measurement, *Nucl. Instrum. Methods Phys. Res. Sect. A* 613 (2) (2010) 257–262.